JACC: CARDIOVASCULAR IMAGING VOL. 4, NO. 6, 2011

ISSN 1936-878X/$36.00
PUBLISHED BY ELSEVIER INC. DOI:10.1016/j.jcmg.2011.03.013

NIRS and IVUS for Characterization of Atherosclerosis in Patients Undergoing Coronary Angiography

Salvatore Brugaletta, MD,*† Hector M. Garcia-Garcia, MD, PhD,*‡
Patrick W. Serruys, MD, PhD,* Sanneke de Boer, MD,* Jurgen Ligthart, BSc,*
Josep Gomez-Lara, MD,* Karen Witberg, RN,* Roberto Diletti, MD,*
Joanna Wykrzykowska, MD,*‖ Robert-Jan van Geuns, MD, PhD,*
Carl Schultz, MD,* Evelyn Regar, MD, PhD,* Henricus J. Duckers, MD, PhD,*
Nicolas van Mieghem, MD,* Peter de Jaegere, MD, PhD,* Sean P. Madden, PhD,§
James E. Muller, MD, PhD,§ Antonius F. W. van der Steen, PhD,*
Wim J. van der Giessen, MD, PhD,* Eric Boersma, PhD*

Rotterdam and Amsterdam, the Netherlands; Barcelona, Spain; and Burlington, Massachusetts

OBJECTIVES The aim of this study was to compare the findings of near-infrared spectroscopy (NIRS), intravascular ultrasound (IVUS) virtual histology (VH), and grayscale IVUS obtained in matched coronary vessel segments of patients undergoing coronary angiography.

BACKGROUND Intravascular ultrasound VH has been developed to add tissue characterization to the grayscale IVUS assessment of coronary plaques. Near-infrared spectroscopy is a new imaging technique able to identify lipid core-containing coronary plaques (LCP).

METHODS We performed NIRS and IVUS-VH pullbacks in a consecutive series of 31 patients with a common region of interest (ROI) between 2 side branches. For each ROI, we analyzed the chemogram blocks by NIRS, plaque area and plaque burden by grayscale IVUS, and tissue types by IVUS-VH. The chemogram block is a summary metric of a 2-mm vertical slice of the chemogram. The value ranges from 0 to 1 according to the presence of lipids and represents the probability of LCP with a color scale from red (low probability) through orange and tan to yellow (high probability).

RESULTS Plaque area (mm^2) increases as percentage VH derived-necrotic core (NC) content (4.6 $\pm$ 2.7 vs. 7.4 $\pm$ 3.5 vs. 8.6 $\pm$ 3.4 vs. 7.9 $\pm$ 3.3, grouped in percentage NC quartiles, $p < 0.001$) and chemogram block probability color bin thresholds increase (4.9 $\pm$ 3.8 red, 7.3 $\pm$ 3.6 orange, 8.1 $\pm$ 3.4 tan, and 8.7 $\pm$ 3.4 yellow, $p < 0.001$). The correlation between the block chemogram detection of lipid core and percentage NC content by VH was weak ($r = 0.149$). Correction for the presence of calcium does not improve this correlation.

CONCLUSIONS Larger plaque area by grayscale IVUS was more often associated with either elevated percentage VH-NC or LCP by NIRS; however, the correlation between the detection of LCP by NIRS and necrotic core by VH is weak. (J Am Coll Cardiol Img 2011;4:647–55) © 2011 by the American College of Cardiology Foundation

From the *Thoraxcenter, Erasmus Medical Center, Rotterdam, the Netherlands; †Department of Cardiology, Thorax Institute, Hospital Clinic, Barcelona, Spain; ‡Cardialysis BV, Rotterdam, the Netherlands; §InfraReDx, Inc., Burlington, Massachusetts; and the ‖Academic Medical Center, Amsterdam, the Netherlands. Drs. Muller and Madden are current employees of InfraReDx, Inc. All other authors have reported that they have no relationships to disclose.

Manuscript received October 18, 2010; revised manuscript received March 7, 2011, accepted March 14, 2011.

Lipid core-containing coronary plaques (LCP) are thought to be a cause of most acute coronary syndromes (ACS) (1,2). Near-infrared spectroscopy (NIRS), which is routinely used in science and industry to determine the chemical composition of substances, has the potential to identify such LCP in vivo, possibly improving patient risk stratification and guiding therapy (3). A novel intracoronary catheter system, that employs NIRS to detect LCP in vivo, has recently been developed. The system was prospectively validated versus histology in a double-blind manner with over 2,500 coronary autopsy sections (4). A clinical trial then documented that similar NIRS spectroscopy data could be acquired in vivo (5).

See page 656

Intravascular ultrasound (IVUS)-based methods have also been developed to detect "necrotic core," a term considered to be synonymous with "lipid core." Necrotic core (NC) by IVUS-virtual histology (VH) has been extensively studied (6) and related to clinical characteristics (7) and cardiovascular risk score (8). Intravascular ultrasound VH has also been used for testing the efficacy of novel therapies (9) and has recently been associated with a higher risk of events in a large trial (10). Although NC detection by IVUS-VH is based on pattern classification of backscattering ultrasound signal (11), LCP detection by NIRS is based on near infrared spectral signals from coronary plaques (4).

ABBREVIATIONS AND ACRONYMS

ACS = acute coronary syndrome(s)
GUI = graphical user interface
IVUS-VH = intravascular ultrasound-virtual histology
LCP = lipid core-containing coronary plaques
NC = necrotic core
NIRS = near-infrared spectroscopy
ROI = region of interest
VH-NC = virtual histology-necrotic core

Therefore, the aim of our study was to explore the relationship between the plaque parameters detected by NIRS (LCP) with those detected by grayscale IVUS (plaque area) and VH (VH components).

METHODS

Population. We prospectively analyzed all the consecutive patients who underwent IVUS-VH and NIRS evaluation in the same artery at our institution (Thoraxcenter, Erasmus Medical Center, Rotterdam, the Netherlands). All patients included were more than 18 years of age, with stable angina pectoris or unstable angina pectoris or with ACS. After percutaneous coronary intervention of the culprit lesion, these patients underwent imaging of a vessel that did not contain the culprit lesion. All the study coronary vessels included were accessible to the IVUS-VH and Lipiscan (InfraReDx, Burlington, Massachusetts) catheters and had a <50% reduction in lumen diameter by angiographic visual estimation throughout a target segment of at least 40 mm in length. Coronary vessels that received a bypass graft (n = 5) with a minimal lumen diameter <2 mm or with a diameter stenosis >50% by angiographic visual estimation in the segments to be analyzed (n = 11) were excluded.

The study was conducted under the supervision of the institutional review board, and a dedicated written informed consent form was required.

Grayscale and radiofrequency IVUS analysis. Radiofrequency-IVUS with a phased-array, 20-MHz, 3.2-F catheter (Eagle Eye, Volcano Corporation, Rancho Cordova, California) was performed. During motorized catheter pullback, at 0.5 mm/s, grayscale-IVUS and raw radiofrequency data capture gated to the R-wave were recorded (s5i system, Volcano Corporation). Radiofrequency-IVUS uses spectral (frequency) analysis as well as amplitude data from the IVUS signal, which have been validated for tissue characterization against histological samples with high sensitivity and specificity (11,12).

All baseline IVUS images were prospectively analyzed offline by independent core laboratory (Cardialysis BV, Rotterdam, the Netherlands). The IVUS analyses were performed with VIAS software (Volcano Corporation). Contour detection was performed by experienced IVUS analysts who were blinded to the NIRS results (13). Quantitative grayscale IVUS measurements included vessel area, lumen area, plaque area (vessel area − lumen area) and plaque burden ([plaque area/vessel area] · 100). For the radiofrequency-IVUS analyses, 4 tissue components (NC—red; dense calcium—white; fibrous—dark green; and fibrofatty—light green) were identified with autoregressive classification systems. Each individual tissue component was quantified and color coded in IVUS cross sections, as previously described (11,14).

NIRS analysis. The NIRS system consists of a 3.2-F rapid exchange catheter, a pullback and rotation device, and a console. A motorized catheter pullback, at 0.5 mm/s, was performed in the same artery as IVUS-VH. During the acquisition, as many landmarks as available were identified by the technicians/physicians, under fluoroscopic guidance, identifying fiducial locations such as side branches. These fiducial locations were documented by means

Table 1. Demographic, Clinical, and Angiographic Characteristics of the Study Patients (n = 31)

Age, yrs	60.4 ± 9.6
Male	26 (83)
Clinical history	
Hyperlipidemia	21 (67)
Hypertension	20 (64)
Diabetes mellitus	5 (16)
Current smoker	18 (58)
Prior MI	16 (51)
Prior PCI	4 (13)
Prior coronary artery bypass graft	3 (9)
Cerebrovascular accident/transient ischemic attack	2 (6)
Family history of coronary artery disease	17 (54)
Congestive heart failure	2 (6)
Clinical presentation	
Post MI	2 (6)
Unstable angina	16 (51)
Stable angina	13 (43)
Vessel investigated by IVUS-VH and NIRS	
LAD	6 (20)
LCx	16 (51)
RCA	9 (29)

Values are mean ± SD or n (%).
IVUS-VH = intravascular ultrasound virtual histology; LAD = left anterior descending artery; LCx = left circumflex artery; MI = myocardial infarction; NIRS = near infrared spectroscopy; PCI = percutaneous coronary interventions; RCA = right coronary artery.

of an angiogram, showing the position of the NIRS probe.

The system acquires approximately 1,000 NIRS measurements/12.5 mm of artery scanned. Each measurement interrogates an approximate volume of 1 to 2 mm^3 of lumen surface perpendicular to the long axis of the catheter and centered on the optical tip of the catheter. The measurement of the probability of LCP for each scanned arterial segment is displayed as a map, with the x-axis indicating the pullback position in millimeters and the y-axis indicating the circumferential position of the measurement in degrees. The entire display is termed "chemogram," with the probability of LCP presence coded on a color scale from red to yellow (0 for red, and 1 for yellow). To enhance interpretation of the chemogram and allow block-by-block comparison with histology (4), a summary metric (the chemogram block) is computed to display the probability that an LCP is present in each 2-mm block of the pullback, without regard to rotation. The chemogram block display in the graphical user interface (GUI) uses a binned color scale: red ($p < 0.57$), orange ($0.57 \leq p < 0.84$), tan ($0.84 \leq p < 0.98$) and yellow ($p \geq 0.98$).

Cross-correlation of the IVUS-VH and NIRS. An independent experienced analyst, blinded to all patient clinical information, used a side-by-side view of both imaging techniques (IVUS-VH and NIRS), color blinded for IVUS-VH data. The cross correlation between the imaging data was obtained by the following 4-step method. First, the landmarks in the NIRS pullback (side branches) were identified in the angiogram. Second, the landmarks in the angiogram and in the NIRS pullback were also identified in the IVUS-VH. Third, the region so identified in NIRS and IVUS-VH pullbacks was defined as our region of interest (ROI). Fourth, the ROI identified in the IVUS-VH was divided into subregions, according to the number of chemogram blocks displayed by NIRS in that ROI (each chemogram block gives information on a region of 2 mm in length), resulting in an average of 4 VH frames/2-mm chemogram block. The percentage content of each VH component for a given collection of frames matched to a chemogram block was done in this manner: [total area of each VH component in those frames/total plaque area in those frames] · 100.

Statistical analysis. Continuous variables are expressed as mean ± SD. The percentage content of NC was divided into quartiles and used as categorical variables. The probability displayed in the chemogram block, that LCP is present, was used as continuous variable (range from 0 to 1) and also transformed into a categorical variable, according to the same values used in the binned

Table 2. Baseline Intracoronary Imaging Data/ROI (n = 31)

Grayscale IVUS and VH data	
Mean vessel area (mm^2)	13.6 ± 6.2
Mean lumen area (mm^2)	7.3 ± 3.1
Plaque burden (%)	39.5 ± 15.6
Mean plaque area (mm^2)	5.9 ± 3.9
Fibrous tissue (%)	55.6 ± 17.9
Fibrofatty tissue (%)	9.1 ± 8.6
NC tissue (%)	22.2 ± 12.1
Dense calcium (%)	12.9 ± 12.2
NIRS data	
Number of blocks/ROI	18 ± 8
Block chemogram value	0.37 ± 0.36
Block chemogram color	
Red	397 (70)
Tan	68 (12)
Orange	42 (7)
Yellow	56 (11)

Values are mean ± SD or n (%).
NC = necrotic core; ROI = region of interest; other abbreviations as in Table 1.

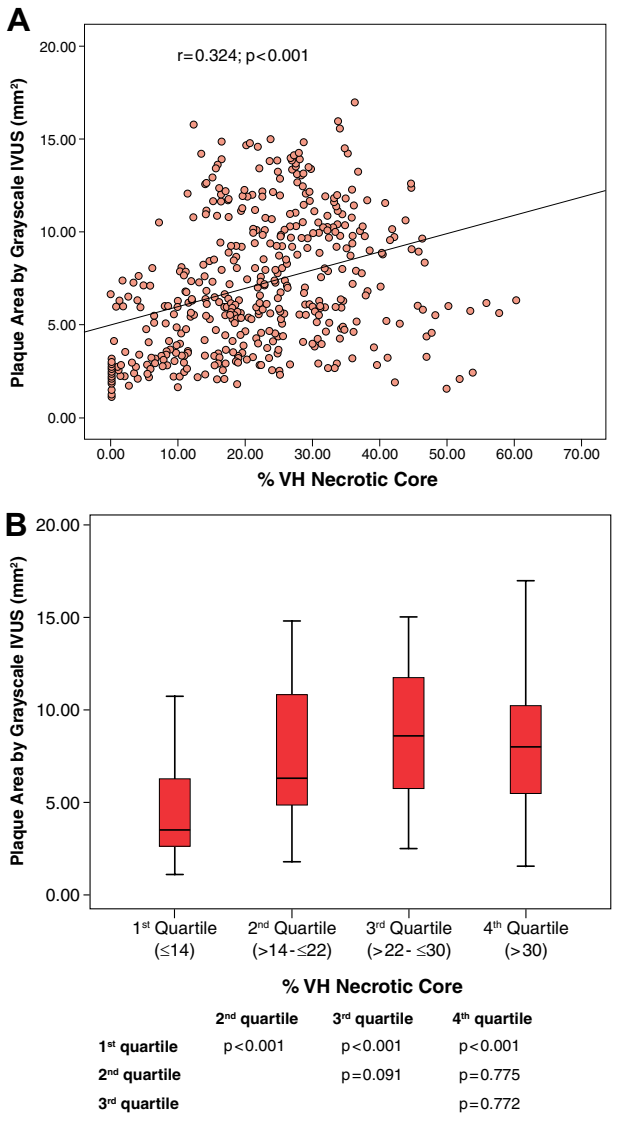

Figure 1. Correlation Between IVUS-Plaque Area and VH-NC

(A) The correlation plot, showing the distribution of plaque area and percentage necrotic core (NC) (Pearson Correlation). **(B)** Grayscale plaque area grouped according to quartiles of percentage content of virtual histology (VH)-NC (p values show the comparison between groups). IVUS = intravascular ultrasound.

color scale of the GUI (red, $p < 0.57$; orange, $0.57 \leq p < 0.84$; tan, $0.84 \leq p < 0.98$; and yellow, $p \geq 0.98$). Comparisons between groups and correlations between variables were applied, depending on normal or non-normal distribution of the variables. Statistical analysis for comparison between groups was also performed, with Bonferroni or Dunn corrections for multiple comparisons. The normal distribution was tested with the Kolmogorov-Smirnov test. No adjustments for patient or frame clustering data have been performed. A probability value <0.05 was considered significant, and all tests were 2-tailed. Data were analyzed with SPSS software (version 16.0, SPSS, Inc., Chicago, Illinois).

RESULTS

Population. A total of 31 patients were included in the present analysis. Table 1 shows baseline clinical characteristics. None of the patients experienced an adverse event due to the imaging acquisition.

Intracoronary imaging data. Overall, the average length of ROI was 36.0 mm, and the mean plaque burden/ROI was 39.5% with a mean value of NC of 22.2%. A mean of 18 block chemograms were identified per each ROI, exhibiting a mean value of 0.37. Most of them (70%) were coded as red in the GUI, although 11% were coded as yellow (Table 2). A total of 563 NIRS chemogram blocks were then matched with VH data.

Correlation between grayscale IVUS plaque area and VH-NC/LCP by NIRS. A large plaque area by grayscale IVUS was more often associated with elevated percentage VH-NC content ($r = 0.324$, $p < 0.001$) (Fig. 1A). In particular, grayscale plaque area, grouped according to quartiles of percentage VH-NC content, was significantly different between the quartiles (4.6 ± 2.7 mm^2 vs. 7.4 ± 3.5 mm^2 vs. 8.6 ± 3.4 mm^2 vs. 7.9 ± 3.3 mm^2, from 1st to 4th quartile, respectively, $p < 0.001$). In further analysis, the p values were statistically significant for the comparison of 1st versus 2nd, 3rd, or 4th quartile, although no differences were found between the other quartiles (Fig. 1B).

A large plaque area by grayscale IVUS was more often associated also with LCP by NIRS ($r = 0.449$, $p < 0.001$) (Fig. 2A). In particular, grayscale plaque area, grouped according to chemogram block probability color bin thresholds, was significantly different between the groups (4.9 ± 3.8 mm^2 red, 7.3 ± 3.6 mm^2 orange, 8.1 ± 3.4 mm^2 tan, and 8.7 ± 3.4 mm^2 yellow, $p < 0.001$). In the analysis comparing the various groups, p values were statistically significant for the comparison between red versus orange, tan, or yellow (Fig. 2B).

Correlation between VH and NIRS. Overall, 365 NC-rich (≥10% of NC% content) VH-frames were identified. Fifty-two of these (14.2%) were coded as yellow by NIRS, although 225 (61.6%) were coded as red by NIRS. Conversely, 4 of 73 NC-poor (<10% of NC content) VH frames by IVUS-VH were coded as yellow by NIRS.

Correlation between percentage VH-NC content of plaque and chemogram block probability was weak (r = 0.149, p = 0.002) (Fig. 3A). The percentage VH-NC content, grouped according to chemogram block probability color bin thresholds, was significantly different between groups (20.6 ± 11.9 red, 23.5 ± 12.8 orange, 23.0 ± 10.7 tan, and 27.1 ± 11.7 yellow, p = 0.002). However, yellow showed a higher percentage VH-NC content compared with red, although no differences were found among the other groups (Fig. 3B).

The correlation between the block chemogram and the total percentage content of VH-NC and fibrofatty tissues was also weak, and the data were widely dispersed (r = 0.252, p < 0.001). Although in the lesions with a percentage content of dense calcium (DC) >10%, the correlation between percentage VH-NC and block chemograms was significant and weak (r = 0.203, p < 0.001), in the lesions with a percentage content of DC <10%, this correlation was not significant (r = 0.130, p = 0.054). In particular, although the block chemogram values were not different between calcified and noncalcified plaques (0.42 ± 0.43 vs. 0.40 ± 0.41, p = 0.484), the percentage VH-NC was significantly higher in calcified plaques, compared with noncalcified plaques (29.0 ± 9.3% vs. 15.5 ± 10.6%, p < 0.001).

Figures 4 and 5 show some cases of agreement and disagreement between the 2 techniques.

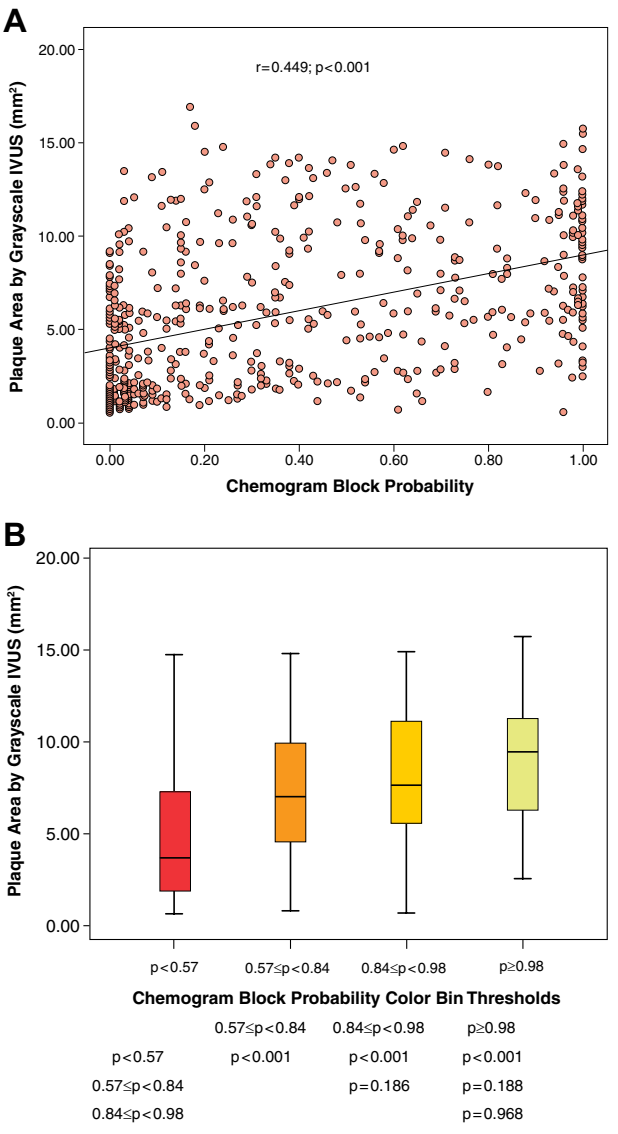

Figure 2. Correlation Between IVUS-Plaque Area and Chemogram Block Probability

(A) The correlation plot, showing the distribution of plaque area and chemogram block probability (Spearman rho). **(B)** Grayscale intravascular ultrasound (IVUS) plaque area (mm^2) grouped according to chemogram block probability color bin thresholds (p values show the comparison between groups).

DISCUSSION

The major findings of our study are: 1) NC-rich VH plaques and LCP identified by NIRS have higher grayscale plaque area than corresponding NC/lipid-poor counterparts; and 2) the correlation between the relative VH-NC content of the plaque and the values of the block chemogram of the NIRS is weak.

Near-infrared spectroscopy and IVUS-VH are 2 intracoronary imaging techniques that allow identification of plaque with high lipid/NC content, interpreting the near infrared spectral signals and the intravascular backscattering coming from the atherosclerotic plaque, respectively. There is an important consideration to make with regard to the validation of these techniques. For the validation of NIRS, a lipid core plaque was defined as a fibroatheroma with lipid core >60° in circumferential extent, >200-μm-thick, with a fibrous cap having a mean thickness <450 μm and correlated with each chemogram block (4). For the validation of IVUS-VH, NC was defined as region comprising cholesterol clefts and foam cells. Some lipid components in the presence of collagen are also coded as fibrofatty tissues (11). This is of critical importance, because it might be the source of their different capabilities of detecting NC/lipid.

In this analysis, we found that plaque area increases with the increase of its VH-NC content (Fig. 1). In addition, it also increases according to the block chemogram value, with the plaques

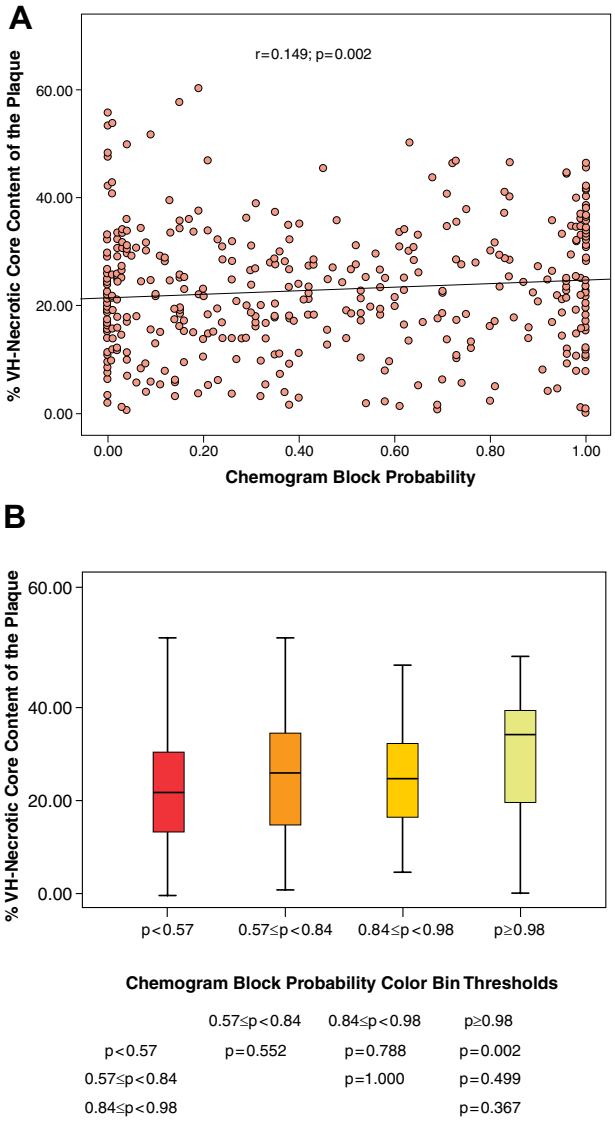

Figure 3. Correlation Between VH-NC and Chemogram Block Probability

(A) The correlation plot, showing the distribution of percentage VH-NC content of the plaque and chemogram block probability (Spearman rho). **(B)** Percentage VH-NC content of plaque, grouped according to chemogram block probability color bin thresholds (p values show the comparison between groups). Abbreviations as in Figures 1 and 2.

coded as yellow by NIRS having larger area, compared with those coded as red (Fig. 2) Plaque area is, indeed, an estimation of severity of atherosclerosis, and we have previously shown that it correlates with VH-NC size (15,16). Although plaque and lipid/necrotic core size are closely related, the PROSPECT (Providing Regional Observations to Study Predictors of Events in the Coronary Tree) trial has shown that both high plaque burden and thin cap NC-rich VH plaques are independent predictors of long-term events in patients after ACS (10).

Of note is that, although plaques coded as yellow by NIRS tend to have higher VH-NC than those coded as red, the data are widely dispersed, and hence, the correlation between the block chemograms and relative VH-NC is weak with low statistical significance. As previously mentioned, VH-fibrofatty tissue also includes some lipid component. However, considering relative VH-NC and VH-fibrofatty tissue together, its correlation with yellow-block chemogram was still weak.

It is also important to highlight that, unlike ultrasound, NIRS signal is not affected by an inability to cross calcium. Dense calcium was shown to have an impact on a possible artifactual measurement of NC tissue by VH (17). In our analysis we confirm this finding, showing a higher percentage VH-NC in the calcified VH lesions (>10% of DC), compared with the less-calcified counterparts, whereas block chemograms were not influenced by the presence of calcium. Excluding calcified lesions from the analysis, a potential source of incorrect classification of NC, the weak correlation between VH-NC and yellow block chemograms did not improve but rather worsened. The weakness of this correlation cannot be fully explained, because a gold-standard, such as histology, is missing in the present study. The fundamental differences in the principles of each technique—VH is based on pattern classification of backscattering ultrasound signal, whereas NIRS is based on near infrared spectral signals—and their respective limitations should be taken into account in the interpretation of this disagreement between NIRS and IVUS-VH.

In addition to incorrect classification of NC behind calcium, VH has other limitations, related to contours drawing (e.g., in presence of side branches) (18,19) and thrombus classification (18). An important consideration is also that the sensitivity and specificity of NC-VH detection is not 100% but is approximately 90% (11,12,20–22).

Conversely, Gardner et al. (4), comparing the chemogram signals and histological findings, reported that false positive reading of NIRS could be caused by fibroatheromas too small or with caps too thick to meet criteria for LCP of interest or by lesions containing significant lipid but not having NC (intimal xanthoma and pathologic intimal thickening). However, such false positives were not a failure of spectroscopy (i.e., lipid was present and generated a NIRS signal). False negative readings, by contrast, were frequently produced by small lipid cores with extensive calcification and probably dis-

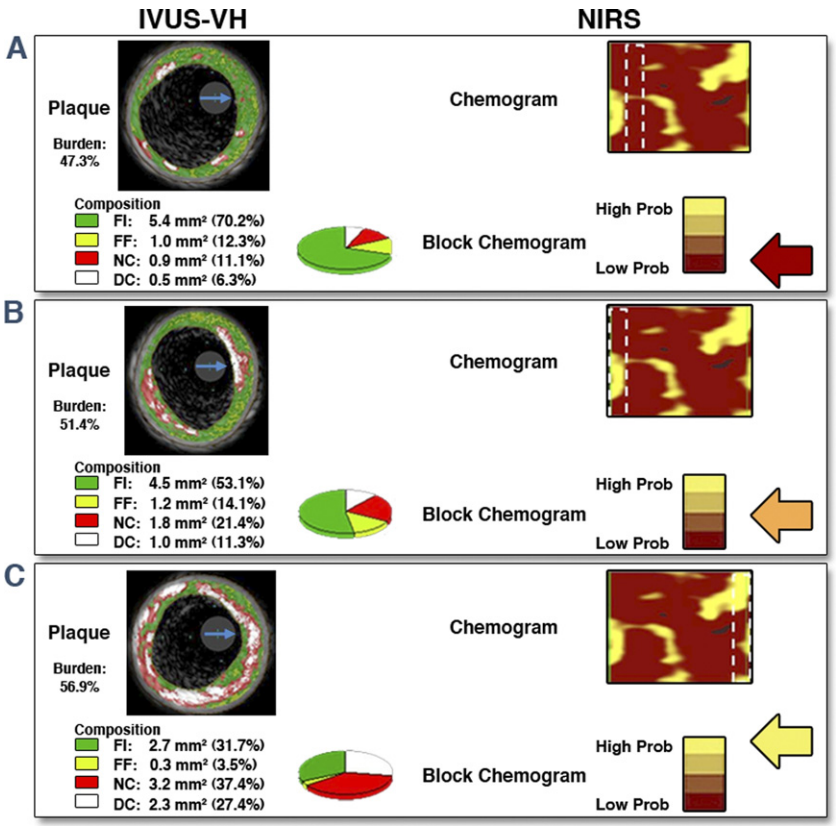

Figure 4. Cases of Agreement Between VH and NIRS

(A) There is no confluent NC in the VH that correlates with a low probability of lipid content by near-infrared spectroscopy (NIRS). **(B)** A VH plaque with moderate amount of NC (from 7 to 9 o'clock) that is confluent in close proximity to the lumen. This correlates with intermediate probability of lipid by NIRS. **(C)** Large confluent area of VH-NC from 7 to 9 o'clock next to a severe calcified region that correlates with a "yellow" NIRS plaque representing high probability for lipid content. DC = dense calcium; FF = fibrofatty tissue; FI = fibrous tissue; other abbreviations as in Figures 1 and 2.

placement of lipid by calcium or from signal obtained in a large lumen in which blood obscures the lipid signal. In addition, we can hypothesize that an eccentric position of the NIRS catheter far away from the plaque together with a fibrous cap too thick to allow the transmission of the NIR signal can explain some cases of disagreement between NIRS and VH.

A large and prospective study is necessary to compare the clinical utility of the information coming from these 2 imaging techniques, because so far neither IVUS-VH nor NIRS could be used to make treatment decisions.

Study limitations. We do not know the exact position of the NIRS catheter inside the vessel (close or far away from the plaque), possibly introducing error into the apparent angular extent of NIRS-identified LCP. A new NIRS catheter (Lipiscan IVUS, InfraReDx) has been developed to simultaneously acquire IVUS and NIRS data, making it possible to correct for this potential distortion (23,24). Although the greatest care was taken to ensure precise collocation of VH and NIRS sections, it is possible that inherent limitations therein played a role in the accuracy of the matching.

We did not explore the relationships among the cap thickness, NIRS, and VH, because other devices—namely optical coherence tomography—provide a more accurate estimation of cap thickness, compared with IVUS-VH.

Finally, the present study compares the results of 3 imaging techniques without comparison with the gold standard of histology.

CONCLUSIONS

The LCP identified by NIRS and NC-rich VH plaques tend to have bigger plaque area (on IVUS grayscale) than corresponding lipid-poor/necrotic core counterparts. However, the correlation be-

JACC: CARDIOVASCULAR IMAGING, VOL. 4, NO. 6, 2011
JUNE 2011:647–55

Figure 5. Cases of Disagreement Between VH and NIRS

We reported some examples of disagreement between VH and NIRS, with some hypothetical explanations. Abbreviations as in Figures 1, 2, and 4.

tween the detection of lipid core rich plaque by NIRS and NC by VH is weak. These findings indicate the need for a similar comparative study of the 2 imaging techniques in autopsy specimens in which the imaging results can be compared with the gold standard of histology. A comparative clinical study in which the ability of either technique to predict clinical outcomes would also be of value.

Reprint requests and correspondence: Dr. Patrick W. Serruys, Thoraxcenter, Ba-583, 's Gravendijkwal 230, 3015 CE, Rotterdam, the Netherlands. *E-mail: p.w.j.serruys@erasmusmc.nl.*

REFERENCES

1. Kolodgie FD, Burke AP, Farb A, et al. The thin-cap fibroatheroma: a type of vulnerable plaque: the major precursor lesion to acute coronary syndromes. Curr Opin Cardiol 2001;16:285–92.
2. Falk E, Shah PK, Fuster V. Coronary plaque disruption. Circulation 1995;92:657–71.
3. Jaross W, Neumeister V, Lattke P, Schuh D. Determination of cholesterol in atherosclerotic plaques with near infrared diffuse reflection spectroscopy. Atherosclerosis 1999;147:327–37.
4. Gardner CM, Tan H, Hull EL, et al. Detection of lipid core coronary plaques in autopsy specimens with a novel catheter-based near-infrared spectroscopy system. J Am Coll Cardiol Img 2008;1:638–48.
5. Waxman S, Dixon SR, L'Allier P, et al. In vivo validation of a catheter-based near-infrared spectroscopy system for detection of lipid core coronary plaques: initial results of the SPECTACL study. J Am Coll Cardiol Img 2009;2:858–68.
6. Burke AP, Kolodgie FD, Zieske A, et al. Morphologic findings of coronary atherosclerotic plaques in diabetics: a postmortem study. Arterioscler Thromb Vasc Biol 2004;24:1266–71.
7. Garcia-Garcia HM, Serruys PW, Mintz GS, et al. Synergistic effect of cardiovascular risk factors on necrotic core in coronary arteries: a report from the global intravascular radiofrequency data analysis registry. J Am Coll Cardiol Img 2009;2:629–36.
8. Marso SP, Frutkin AD, Mehta SK, et al. Intravascular ultrasound measures of coronary atherosclerosis are associated with the Framingham risk score: an analysis from a global IVUS registry. EuroIntervention 2009;5:212–8.
9. Serruys PW, Garcia-Garcia HM, Buszman P, et al. Effects of the direct lipoprotein-associated phospholipase A(2) inhibitor darapladib on human coronary atherosclerotic plaque. Circulation 2008;118:1172–82.
10. Stone GW, Maehara A, Lansky AJ, et al. A prospective natural-history study of coronary atherosclerosis. N Engl J Med;364:226-35.

11. Nair A, Kuban BD, Tuzcu EM, Schoenhagen P, Nissen SE, Vince DG. Coronary plaque classification with intravascular ultrasound radiofrequency data analysis. Circulation 2002;106:2200–6.
12. Nair A, Margolis MP, Kuban BD, Vince DG. Automated coronary plaque characterisation with intravascular ultrasound backscatter: ex vivo validation. EuroIntervention 2007;3:113–20.
13. Hausmann D, Lundkvist AJ, Friedrich GJ, Mullen WL, Fitzgerald PJ, Yock PG. Intracoronary ultrasound imaging: intraobserver and interobserver variability of morphometric measurements. Am Heart J 1994;128:674–80.
14. Serruys PW, Ormiston JA, Onuma Y, et al. A bioabsorbable everolimus-eluting coronary stent system (ABSORB): 2-year outcomes and results from multiple imaging methods. Lancet 2009;373:897–910.
15. Garcia-Garcia HM, Goedhart D, Serruys PW. Relation of plaque size to necrotic core in the three major coronary arteries in patients with acute coronary syndrome as determined by intravascular ultrasonic imaging radiofrequency. Am J Cardiol 2007;99:790–2.
16. Qian J, Maehara A, Mintz GS, et al. Relation between individual plaque components and overall plaque burden in the prospective, multicenter virtual histology intravascular ultrasound registry. Am J Cardiol 2009;104:501–6.
17. Sales FJ, Falcao BA, Falcao JL, et al. Evaluation of plaque composition by intravascular ultrasound "virtual histology": the impact of dense calcium on the measurement of necrotic tissue. EuroIntervention 2010;6:394–9.
18. Garcia-Garcia HM, Mintz GS, Lerman A, et al. Tissue characterisation using intravascular radiofrequency data analysis: recommendations for acquisition, analysis, interpretation and reporting. EuroIntervention 2009;5:177–89.
19. Shin ES, Garcia-Garcia HM, Serruys PW. A new method to measure necrotic core and calcium content in coronary plaques using intravascular ultrasound radiofrequency-based analysis. Int J Cardiovasc Imaging;26:387–96.
20. Thim T, Hagensen MK, Wallace-Bradley D, et al. Unreliable assessment of necrotic core by virtual histology intravascular ultrasound in porcine coronary artery disease. Circ Cardiovasc Imaging 2010;3:384–91.
21. Granada JF, Wallace-Bradley D, Win HK, et al. In vivo plaque characterization using intravascular ultrasound-virtual histology in a porcine model of complex coronary lesions. Arterioscler Thromb Vasc Biol 2007;27:387–93.
22. Nasu K, Tsuchikane E, Katoh O, et al. Accuracy of in vivo coronary plaque morphology assessment: a validation study of in vivo virtual histology compared with in vitro histopathology. J Am Coll Cardiol 2006;47:2405–12.
23. Schultz CJ, Serruys PW, van der Ent M, et al. First-in-man clinical use of combined near-infrared spectroscopy and intravascular ultrasound: a potential key to predict distal embolization and no-reflow? J Am Coll Cardiol 2010;56:314.
24. Garg S, Serruys PW, van der Ent M, et al. First use in patients of a combined near infra-red spectroscopy and intra-vascular ultrasound catheter to identify composition and structure of coronary plaque. EuroIntervention 2010;5:755–6.

Key Words: intravascular ultrasound ■ near-infrared spectroscopy ■ virtual histology.